

Lithium in strong magnetic fields

Omar-Alexander Al-Hujaj*

Theoretische Chemie, Institut für Physikalische Chemie der Universität Heidelberg, INF 229, 69120 Heidelberg, Germany

Peter Schmelcher†

*Theoretische Chemie, Institut für Physikalische Chemie der Universität Heidelberg, INF 229, 69120 Heidelberg, Germany and
Physikalisches Institut der Universität Heidelberg, Philosophenweg 12, 69120 Heidelberg, Germany*

(Dated: March 16, 2018)

The electronic structure of the lithium atom in a strong magnetic field $0 \leq \gamma \leq 10$ is investigated. Our computational approach is a full configuration interaction method based on a set of anisotropic Gaussian orbitals that is nonlinearly optimized for each field strength. Accurate results for the total energies and one-electron ionization energies for the ground and several excited states for each of the symmetries $^20^+$, $^2(-1)^+$, $^4(-1)^+$, $^4(-1)^-$, $^2(-2)^+$, $^4(-2)^+$, $^4(-3)^+$ are presented. The behaviour of these energies as a function of the field strength is discussed and classified. Transition wave lengths for linear and circular polarized transitions are presented as well.

PACS numbers: 32.60+i, 32.30.-r, 32.70.-n

I. INTRODUCTION

During the past twenty years an enormous development of our knowledge on atoms exposed to strong magnetic fields has taken place (see the reviews [1, 2, 3, 4, 5] and references therein). Focusing on astrophysical conditions and on the field regime $100 \leq B \leq 10^5$ T for magnetic white dwarfs it is in particular the one and two-electron problems, i.e. the hydrogen and helium atom, whose behavior and properties in strong magnetic fields have been investigated in detail. In both cases our knowledge on the electronic structure of the atoms has had major impact on astrophysical observation. For the hydrogen atom a huge amount of data is nowadays available both with respect to the bound state energy levels and transition moments [2] as well as for the continuum properties [6]. Among others, the corresponding data have lead to a conclusive interpretation of the observed spectrum of the white dwarf GrW+70°8247 which was a key to our understanding of the properties of spectra of magnetic white dwarfs in general (see e.g. Refs. [7, 8, 9, 10, 11]).

In the late nineties a powerful computational approach was developed and implemented in order to study many-electron atomic problems in the presence of a strong magnetic field. During the past six years this approach was applied in order to investigate the electronic structure of the helium atom thereby covering the complete regime of astrophysically relevant field strengths [12, 13]. Approximately 90 excited electronic states are now known with high accuracy thereby yielding 12000 transition wavelengths. As a consequence strong evidence arose that the mysterious absorption edges of the magnetic white dwarf GD229 [14, 15, 16], which were for almost 25 years

unexplained, are due to helium in a strong magnetic field $B \approx 50\,000$ T [17, 18]. Also very recently the newly established helium data were used to analyze a number of magnetic and suspected-magnetic southern white dwarfs [19, 20].

Although our knowledge on the electronic structure of hydrogen and helium in a strong magnetic field have allowed for the interpretation of absorption features of a variety of magnetic white dwarfs, there are other magnetic objects whose spectra can not be explained in terms of these species. In addition, due to the increasing availability of observatories with higher resolutions and sensitivities, new spectra have been obtained that remain unexplained [21], thereby opening the necessity for studies of heavier atoms exposed to magnetic fields: The ongoing Sloan Digital Sky Survey already doubled the number of known magnetic white dwarfs [22]. It is believed that these heavy atoms are present in the atmospheres of the corresponding stars due to accretion of interstellar matter, and particularly it is expected that these objects are quite common [23]. In spite of this interest in multi-electron atoms in strong magnetic fields there is only a very scarce literature. One reason for this is certainly the conceptual and computational difficulties associated with the competing electron-electron, electron-nuclear-attraction, paramagnetic and diamagnetic interactions which are of comparable strength under astrophysical conditions.

The present work makes a start to fill the above-mentioned gap and develops a full configuration interaction (full CI) approach for multi-electron systems thereby focusing on the lithium atom in a strong magnetic field. Let us comment at this point on the state-of-the-art of the literature on the lithium atom exposed to the field thereby following a chronological order. In Ref. [24] a combination of an adiabatic and Hartree-Fock (HF) approach is employed to obtain ground state energies for four different field strengths in the high field regime. Ref. [25] provides also values of the ground state energy

*Electronic address: Alexander.Al-Hujaj@pci.uni-heidelberg.de

†Electronic address: Peter.Schmelcher@pci.uni-heidelberg.de

via a HF adiabatic approach in the high field regime. Ref. [26] equally employs an unrestricted HF approach in order to obtain the energies of the ground states of the symmetry subspaces 2^0+ , $2^2(-1)^+$, $4^4(-1)^+$, $4^4(-1)^-$ for the weak to intermediate regime of field strengths $\gamma = 0 - 5$ (γ denotes the magnetic field strength in atomic units, where $\gamma = 1$ corresponds to $2.355 \cdot 10^5$ T). Ref. [27] contains also a HF investigation of the 1^20+ , $1^2(-1)^+$, $1^4(-1)^+$, $1^2(-1)^-$, $1^4(-3)^+$ electronic states in the complete regime $\gamma = 0 - 1000$. Neutral atoms for nuclear charge numbers $Z = 1 - 10$ in the high field regime are investigated in Ref. [28] equally within a HF approach. The crossovers of the symmetries of the ground states are discussed and analyzed in detail. Ref. [29] uses a so-called frozen-core approach to simplify the three-electron problem in a strong magnetic field. This was the first fully correlated approach to the lithium atom although it is only valid, i.e. reliable, for not too strong magnetic fields. The three energetically lowest states of 2^0+ , $2^2(-1)^+$, $2^2(-2)^+$ symmetry have been studied for the regime $\gamma = 0 - 5.4$. More recently [30] adds to these results a denser grid of field strengths for the same regime of field strengths and provides also a few oscillator strengths of the corresponding transitions. Finally [31] provides some results on the ground state energies of neutral atoms $Z = 1 - 26$ for a few field strengths.

The present investigation goes in several respects significantly beyond the results in the existing literature on lithium in a strong magnetic field. First of all it covers the complete weak to intermediate regime of field strengths $\gamma = 0 - 10$ and more importantly we provide accurate results of the energies and transition wave lengths for many excited states that have not been studied so far employing a fully correlated approach. The ground and many excited states for each of the symmetry subspaces 2^0+ , $2^2(-1)^+$, $4^4(-1)^+$, $4^4(-1)^-$, $2^2(-2)^+$, $4^4(-2)^+$, $4^4(-3)^+$ are investigated thereby yielding a total of 28 states and their behavior as a function of the field strength for a grid of 11 field strengths in the above-mentioned regime. This multiplies the existing knowledge on the electronic structure of the lithium atom in strong fields.

In detail we proceed as follows. Section II provides the electronic Hamiltonian and discusses its symmetries. Section III contains a description of our full configuration interaction approach and its implementation as well as remarks on the basis set of nonlinearly optimized anisotropic Gaussian orbitals. Section IV, which is the central part of this work, presents the results i.e. the total and ionization energies for the ground and many excited states for a variety of symmetries. Section V yields the wavelengths of the electromagnetic transitions. We close with a summary in section VI.

II. HAMILTONIAN AND SYMMETRIES

The starting point of our investigations is the electronic Hamiltonian for infinite nuclear mass, which takes

in atomic units (a.u.) and for the symmetric gauge of the vector potential the following form:

$$H(\mathbf{B}) = \sum_{i=1}^3 H_i(\mathbf{B}) + \frac{1}{2} \sum_{i \neq j} H_{ij} \quad \text{with} \quad (1)$$

$$H_i(\mathbf{B}) = \frac{\mathbf{p}_i^2}{2} + \frac{\mathbf{B} \cdot \mathbf{l}_i}{2} + \frac{(\mathbf{B} \times \mathbf{r}_i)^2}{8} - \frac{3}{|\mathbf{r}_i|} + \frac{g\mathbf{B} \cdot \mathbf{s}_i}{2} \quad (2)$$

$$H_{ij} = \frac{1}{|\mathbf{r}_i - \mathbf{r}_j|} \quad (3)$$

Here $H_i(\mathbf{B})$ represents the one-particle Hamiltonian of the i -th particle and H_{ij} is the two-particle interaction between particles i and j . Specifically $H_i(\mathbf{B})$ contains the Zeeman-term $1/2 \mathbf{B} \cdot \mathbf{l}_i$, which represents the interaction of the magnetic field with the angular momentum of the electron, the diamagnetic term $1/8(\mathbf{B} \times \mathbf{r}_i)^2$, the Coulomb interaction with the nuclear charge $-3/|\mathbf{r}_i|$, and the spin Zeeman-term $g/2 \mathbf{B} \cdot \mathbf{s}_i$. The two-particle operators represents the electron-electron Coulomb repulsion.

If the magnetic field is chosen to point in z direction, the component of the total angular momentum along the z -axis M , the total spin S , the z projection of the total spin S_z , and the total z parity Π_z are conserved. In the following we use the spectroscopic notation $\nu^{2S+1}M^{\Pi_z}$ for the electronic states. Here ν stands for the degree of excitation, with respect to the specified symmetry. In the following all total energies are given for the spin being maximal polarized antiparallel to the direction of the magnetic field (i.e. $S_z = -S$). Energies for other spin projections can be obtained by adding the corresponding spin Zeeman-energy difference.

III. NUMERICAL METHOD

The Schrödinger equation is solved by applying a full CI approach. The basic ingredient is an anisotropic Gaussian basis set, which was put forward by Schmelcher and Cederbaum [32], and which has been successfully applied to several atoms, ions and molecules [12, 13, 33, 34]. The corresponding basis functions have been optimized for each field strength, and each symmetry separately, in order to solve different one- and two-particle problems, i.e. H, Li^+ , and Li^{2+} , in a magnetic field of the corresponding strength. Therefore a nonlinear optimization procedure has been applied, which has been worked out in our group (see Refs. [12, 13]).

Our lithium calculations have been performed using a configurational basis set of three-electron Slater determinants. The latter are constructed from the canonical orthogonal one-particle basis set (see Ref. [35]), which is obtained by the following cut-off technique. In the first step the overlap matrix $\mathbf{S}(m_j, \pi_{z_j})$ of the primitive Gaussian orbitals is constructed. Its eigenvectors $\{\mathbf{v}_{s_j}(m_j, \pi_{z_j})\}$ and corresponding eigenvalues $\{e_{s_j}(m_j, \pi_{z_j})\}$ are determined. For the following calculations we restrict the number of eigenvectors \mathbf{v}_{s_j} , to those which possess eigenvalues e_{s_j} above an appropriate chosen threshold ε . This

way we avoid quasi-linear dependencies in the configuration space generated by our optimized basis set. With the remaining vectors \mathbf{v}_{s_k} the Schrödinger equation for the one-particle Hamiltonian $H_i(\mathbf{B})$ is mapped on an ordinary matrix eigenvalue problem. The latter is solved numerically and the resulting eigenvectors $\{\mathbf{h}_i(m_j, \pi_{z_j})\}$ serve as the spatial part of our one-particle basis set for the electronic structure calculations. The spinors χ_j are products of this orthogonal one-particle basis functions $\mathbf{h}_i(m_j, \pi_{z_j})$ and the usual spin eigenfunctions α or β . Three-electron Slater determinants are constructed from spinors obeying the correct symmetries, i.e.

$$m_1 + m_2 + m_3 = M \quad (4)$$

$$\pi_{z_1} \pi_{z_2} \pi_{z_3} = \Pi_z \quad (5)$$

$$s_{z_1} + s_{z_2} + s_{z_3} = S_z. \quad (6)$$

In order to keep the one-particle basis set as small as possible, an appropriate selection scheme for the basis functions is crucial. This concerns the selection of the symmetries of the one-particle functions as well as the selection from appropriate sets of orbitals, which result from the above mentioned nonlinear optimizations.

In general the core electrons of doublet states of the lithium atom, i.e. the $1s^2$ configuration, are well described by functions optimized for the $\text{Li}^+ 1^10^+$ state. Therefore we applied a two-particle optimization procedure to functions with the one-particle symmetries $m^{\pi_z} = 0^+$ and $m^{\pi_z} = 0^-$. Further orbitals involved in the calculation of the doublet states of the lithium atom are obtained by optimizing orbitals for the hydrogen atom $Z = 1$.

For the fully spin-polarized quartet states, the situation is different. Electrons are much less correlated and therefore the computationally demanding two-particle optimizations are not truly necessary. Core electrons, i.e. $m^{\pi_z} = 0^+$ and $m^{\pi_z} = 0^-$ are described by functions optimized for Li^{2+} , energetically higher orbitals such as $m^{\pi_z} = (\pm 1)^+$, $m^{\pi_z} = (\pm 1)^-$ are taken from basis sets optimized for $Z = 2$, others from basis sets optimized for $Z = 1$.

Typically the one-particle basis sets consist of approximately 100 Gaussian functions, which give rise to 8 000 – 40 000 three-electron Slater-determinants, depending on the addressed symmetry subspace. Very sophisticated algorithms allow to calculate the full Hamiltonian matrix efficiently. We exploit the fact, that the Hamiltonian matrix is a sparse and symmetric one and apply a Lanczos algorithm for its diagonalization.

IV. TOTAL AND IONIZATION ENERGIES

A. Total energies and global ground states

The symmetries of the global ground states of individual atoms or ions change depending on the field strength [27, 28, 37, 38, 39]: In different field regimes eigenstates

with different symmetries represent the ground state of the system. Therefore the global ground state of an atom or ion experiences a series of crossovers. These crossovers emerge to the delicate interplay between the different terms of the Hamiltonian in the field such as the spin Zeeman, diamagnetic and Coulomb interaction. Of particular importance are here the magnetically tightly bound orbitals that represent a key ingredient of strongly bound atomic or ionic states in strong fields. The number of ground state crossovers for a certain atom or ion in the field cannot be predicted e.g. on the grounds of symmetry reasoning but has to be determined through electronic structure calculations in the presence of the field. The above holds in particular for the lithium atom considered here.

The total energies of the components of the global electronic ground state for lithium as a function of the field strength are depicted in Fig. 1. For $\gamma = 0$ and in the low field regime $0 < \gamma \leq 0.1929$ the state 1^20^+ represents the ground state. It is a doubly tightly bound state, i.e. it involves two tightly bound orbitals of $1s$ character (although we are employing full CI calculations here, we will occasionally use the mean-field (HF) orbital notation to elucidate the character of the fully correlated atomic wave function). For doublet states ($S_z = -1/2$), the total energy decreases for weak fields, due to the spin Zeeman-term, and it increases for strong fields, which is a consequence of the predominance of the increasing (positive definite) kinetic energy. For the 1^20^+ state the total energy passes through a minimum at $\gamma \approx 0.304$ a.u. In the intermediate field regime ($0.1929 \leq \gamma \leq 2.210$) the ground state of the lithium atom is represented by the triply tightly bound state $1^2(-1)^+$, which contains in particular the dominant $1s^22p_{-1}$ configuration. Fig. 1 shows, that the total energy of this state also passes through a minimum, which is at higher field strengths ($\gamma \approx 1.466$), compared to the position of the minimum of the low field ground state. The total energy of the triply tightly bound quartet state $1^4(-3)^+$, which represents the ground state of the lithium atom for high field strengths ($\gamma > 2.210$), is dominated by the spin Zeeman-term ($S_z = -3/2$). This results in a monotonously decreasing total energy.

Our values for the field strengths corresponding to the crossovers of the global ground state deviate about 10% from previously published values for the first crossover and approximately 3% for the second crossover. Ivanov (HF calculations) [27] states for the first crossing field $\gamma 0.17633$ and Guan (modified full core plus correlation method) 0.1753 [30]. The field strength belonging to the second crossover is found by Ivanov at $\gamma = 2.153$ compared to our value of 2.210.

B. Ionization threshold

In order to calculate one-particle binding energies the ionization threshold has to be defined. In the following,

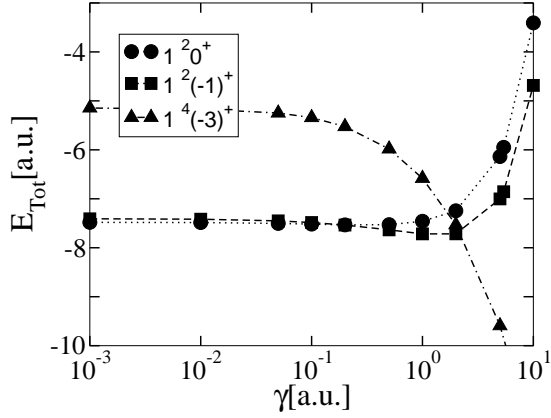


FIG. 1: Total energies E_{Tot} of the global ground states of the lithium atom in a.u. as function of the magnetic field strength γ .

we will define one-particle ionization as a process, that brings one electron to infinity and thereby conserving all quantum numbers of the atomic state. The one-particle ionization threshold $E_T(M, S_z)$ for a state with magnetic quantum number M and z projection S_z of the total spin is defined in the following way:

$$E_T(M, S_z) = \min_{M_1, S_{z_1}} E^{\text{Li}^+}(M_1, S_{z_1}) + E^{e^-}(M_2, S_{z_2}) \quad (7)$$

where $E^{\text{Li}^+}(M_1, S_{z_1})$ and $E^{e^-}(M_2, S_{z_2})$ are the total energies of the Li^+ ion and the electron, respectively, depending on their magnetic quantum numbers M_i and z projection S_{z_i} ($i = 1, 2$) of the total spin. The quantum numbers for the electron M_2 and S_{z_2} can be expressed in terms of the ionic and the atomic quantum numbers

$$M_2 = M - M_1 \quad S_{z_2} = S_z - S_{z_1}. \quad (8)$$

This procedure has to be repeated for each symmetry and field strength in order to identify the corresponding threshold. Therefore several energy levels of Li^+ have to be considered as a function of the field strength. Table I shows the total energies for the Li^+ states, associated to one-particle ionization thresholds.

In the following, we will present our results for the total energies and the one-particle ionization energies for a variety of states of the lithium atom with different symmetries.

C. The symmetry subspace 2^0+

We present in Fig. 2 the one-particle ionization energies for the $\nu^2 0^+$ states ($\nu = 1, 2, 3, 4$), and in table II numerical values for the corresponding total energies, one-particle ionization energies, including previously published data for the total energies. The ionization threshold for these and for all other considered doublet states, is associated with the Li^+ state $1^1 0^+$.

	$1^1 0^+$	$1^3 0^+$	$1^3 (-1)^+$
γ	E_{tot} [a.u.]	E_{tot} [a.u.]	E_{tot} [a.u.]
0.000	-7.277191	-5.110633	-5.026321
0.001	-7.277189	-5.111640	-5.027815
0.010	-7.277327	-5.120614	-5.041247
0.020	-7.277376	-5.110313	-5.056040
0.050	-7.277336	-5.159107	-5.099595
0.100	-7.276897	-5.204480	-5.169539
0.200	-7.274673	-5.286753	-5.300455
0.500	-7.259522	-5.483980	-5.643726
1.000	-7.205547	-5.727321	-6.119216
2.000	-7.004453	-6.126974	-6.899768
5.000	-5.891947	-7.170075	-8.636273
5.400	-5.704147	-7.292325	-8.827671
10.000	-3.153453	-8.490652	-10.659060

TABLE I: Total energies for Li^+ associated to one-particle ionization thresholds at different field strengths for the considered lithium states.

The energetically lowest of the states in the 2^0+ symmetry subspace, represents as mentioned above the global ground state of the atom for low magnetic field strengths. Comparing the total energies to the previously published data, shows, that the relative accuracy for $\gamma = 0$ for the ground state is $4 \cdot 10^{-5}$, $5 \cdot 10^{-4}$ for the state 2^0+ , and $4 \cdot 10^{-3}$ for the 3^0+ state. For finite field strengths our results are significantly below the Hartree-Fock results [26, 27] and at least for $\gamma \geq 0.1$ below the correlated results of Guan [30].

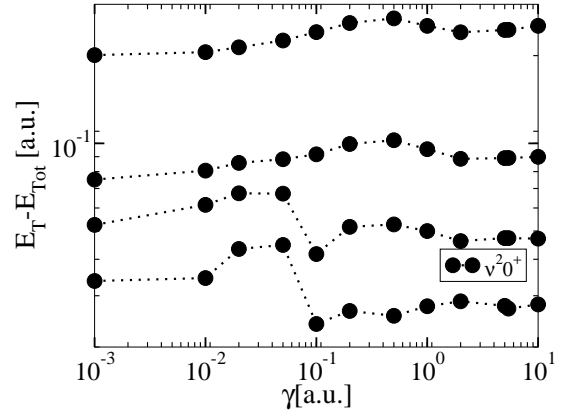


FIG. 2: One-particle ionization energies for the states $\nu^2 0^+$ ($\nu = 1, 2, 3, 4$) as a function of the magnetic field strength γ .

In Fig. 2 it can be seen, that the one-particle ionization energy of the ground state only weakly depends on the field strength. For a vanishing field it amounts to 0.20058 a.u., whereas at a field strength of $\gamma = 10$ it is 0.25310 a.u. It increases for weak to intermediate field strengths and possesses a maximum in the intermediate field regime. A similar statement holds for the first excited state of this symmetry subspace, i.e. for the state

2^20^+ . The one-particle ionization energies for the states 3^20^+ and 4^20^+ exhibit a more pronounced dependence on the field strength. This is especially true in the intermediate field regime, where an avoided crossing between the 2^20^+ , 3^20^+ and 4^20^+ occurs.

D. The symmetry subspace $\nu^2(-1)^+$

The ground state of the symmetry subspace $2^2(-1)^+$ represents the global ground state of the lithium atom in the intermediate field regime. It is a triply tightly bound state being predominantly described by the orbitals $1s^22p_{-1}$. Therefore its one-particle ionization energy increases much more rapidly with increasing field strength, than the corresponding energy of the low field ground state 1^20^+ . This is shown in Fig. 3 and numerical values for the states $\nu^2(-1)^+$ ($\nu = 1, 2, 3, 4$) are listed in Tab. III. Compared to the accurate, zero field results of Sims [43], it can be seen, that the relative accuracy for the states $1^2(-1)^+$, $2^2(-1)^+$, and $3^2(-1)^+$ is about $4 \cdot 10^{-4}$. For finite fields the comparison of the total energies for the $1^2(-1)^+$ state is as follows: our energies are significantly below the Hf energies [27], for $\gamma < 0.5$ above the correlated results in Ref. [30] and for $\gamma \geq 0.5$ below them.

Furthermore the table III shows, that the state $1^2(-1)^+$ becomes for $\gamma \geq 0.2$ the most tightly bound state, i.e. the state with the highest one-particle ionization energy. This holds even for high fields, although there the quartet states have a much lower total energy. For the state $1^2(-1)^+$ the one-particle ionization energy increases about more than one order of magnitude in the considered field range: 0.129935 a.u. at zero magnetic field, and 1.530623 a.u. at $\gamma = 10$.

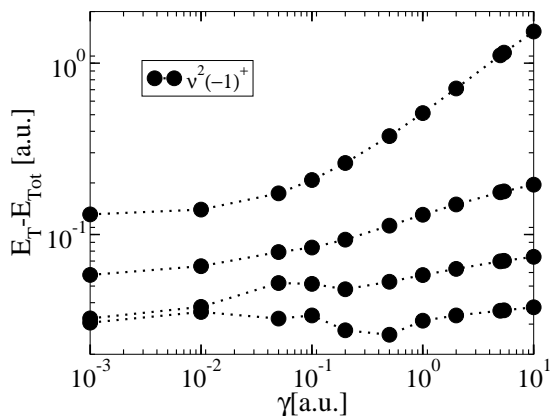


FIG. 3: One-particle ionization energies for the states $\nu^2(-1)^+$ ($\nu = 1, 2, 3, 4$) in a.u. as a function of the magnetic field strength γ .

The one-particle ionization energy of the first excited state $2^2(-1)^+$ increases also monotonously as a function of the field strength. At $\gamma = 0$ it is 0.05581 a.u., for

$\gamma = 10$ it becomes 0.19525 a.u. and therefore increases almost by a factor of 4. For the higher excited states $3^2(-1)^+$ and $4^2(-1)^+$ the effect of an avoided crossing can be observed. Therefore the one-particle ionization energies of these states show a more complex behavior. As a result their ionization energy increases from $\gamma = 0$ to $\gamma = 10$ to a much lower extent, than the ionization energy for the ground and the first excited state.

E. The symmetry subspace $4^4(-1)^+$

Our results for the symmetry subspace $4^4(-1)^+$ are presented in Fig. 4 and in table IV. The spin Zeeman-term causes the total energies of all these fully spin polarized quartet states, to decrease monotonously. On the other hand, this is not reflected by the one-particle ionization energies, which increase or decrease weakly. The ground state $1^4(-1)^+$ is a doubly tightly bound state predominantly consisting of the configuration $1s2s2p_{-1}$. An increase of the one-particle ionization energy can be observed in the field regime $\gamma < 0.2$, which is similar to the increase in the ionization energy for the triply tightly bound state $1^2(-1)^+$. However, in the field regime $\gamma \geq 0.5$ the ionization energy of the state $1^4(-1)^+$ decreases. The reason for this are different one-particle ionization thresholds in the different field regimes. For weak field strengths the ionization threshold involves the Li^+ state 1^30^+ , which is a singly tightly bound state, whereas for $\gamma > 0.2$ it is the $1^3(-1)^+$ state of the Li^+ ion which is a doubly tightly bound state.

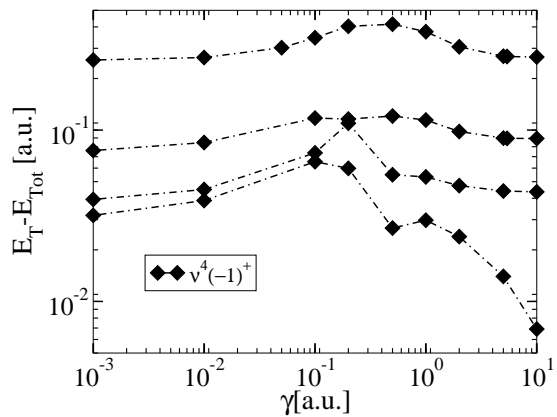


FIG. 4: One-particle ionization energy for the states $\nu^4(-1)^+$ ($\nu = 1, 2, 3, 4$) in a.u. as a function of the magnetic field strength γ .

The decrease in the one-particle ionization threshold can be also observed for the higher excited states of this symmetry ($\nu^4(-1)^+$ with $\nu = 2, 3, 4$). Additional avoided crossings cause the one-particle ionization energies of the states $3^4(-1)^+$ and $4^4(-1)^+$ to decrease. This is very impressive for the state $4^4(-1)^+$, for which the ionization energy at $\gamma = 0.1$ is 0.065426 a.u. and decreases about

$1^2 0^+$			$2^2 0^+$			$3^2 0^+$		$4^2 0^+$	
γ	E_{tot}	E_{Ion}	E_{Lit}	E_{tot}	E_{Ion}	E_{tot}	E_{Ion}	E_{tot}	E_{Ion}
0.000	-7.477766	0.200575	-7.47806032310 ^a	-7.350744	0.073553	-7.304474	0.0272828	-7.280117	0.002925
0 (Lit)				-7.354076 ^e		-7.3355235 ^f		-7.318315 ^e	
0.001	-7.478032	0.200843	-7.43326 ^b	-7.352286	0.075097	-7.329739	0.052550	-7.310861	0.033672
0.010	-7.482888	0.205562	-7.43760 ^b	-7.357941	0.080615	-7.338823	0.061497	-7.311831	0.034505
0.020	-7.490983	0.213607	-7.44214 ^b	-7.363118	0.085743	-7.344767	0.067391	-7.320737	0.043361
0.050	-7.502724	0.213607		-7.365504	0.088169	-7.344529	0.067193	-7.322185	0.044850
0.100	-7.517154	0.240838	-7.5137817 ^c	-7.367564	0.090667	-7.317517	0.040620	-7.300920	0.024023
0.200	-7.533495	0.258822	-7.48400 ^b	-7.374189	0.099516	-7.326335	0.051662	-7.301269	0.026596
0.500	-7.528055	0.268532	-7.5235946 ^c	-7.361991	0.102469	-7.312259	0.052736	-7.285148	0.025626
1.000	-7.458550	0.253003	-7.40879 ^b	-7.301070	0.095523	-7.255573	0.050026	-7.233152	0.027605
2.000	-7.244919	0.240466	-7.19621 ^b	-7.092907	0.088454	-7.050638	0.046185	-7.033148	0.028695
5.000	-6.136918	0.244971	-6.08811 ^b	-5.980919	0.088972	-5.939235	0.047289	-5.919658	0.027712
5.400	-5.949297	0.245150	-5.8772 ^d	-5.793212	0.089065	-5.751426	0.047279	-5.731222	0.027075
10.00	-3.406556	0.253103	-3.35777 ^b	-3.243308	0.089855	-3.200544	0.047091	-3.181432	0.027979

TABLE II: Total energies E_{Tot} , one-particle ionization energies E_{Ion} and previously published results for the total energies E_{Lit} at different field strengths γ in a.u. for the states $\nu^2 0^+$ ($\nu = 1, 2, 3, 4$).

^aRef. [40]

^bRef. [27]

^cRef. [30]

^dRef. [26]

^eRef. [41]

^fRef. [42]

$1^2(-1)^+$				$2^2(-1)^+$			$3^2(-1)^+$			$4^2(-1)^+$	
γ	E _{tot}	E _{Ion}	E _{Lit}	E _{tot}	E _{Ion}	E _{Lit}	E _{tot}	E _{Ion}	E _{Lit}	E _{tot}	E _{Ion}
0.000	-7.407126	0.129935	-7.41016 ^a	-7.334196	0.057005	-7.33716 ^a	-7.307804	0.030612	-7.31190 ^a	-7.306793	0.029602
0.001	-7.408174	0.130986	-7.36609 ^b	-7.335244	0.058055		-7.309562	0.032373		-7.307796	0.030607
0.010	-7.416994	0.139667	-7.37481 ^b	-7.342662	0.065336		-7.315155	0.037828		-7.312592	0.035266
0.050	-7.451086	0.173750		-7.356351	0.079016		-7.329477	0.052141		-7.309611	0.032275
0.100	-7.484773	0.207876	-7.4869343 ^c	-7.360814	0.083917		-7.328362	0.051465		-7.310557	0.033660
0.200	-7.536032	0.261359	-7.49220 ^b	-7.367931	0.093258		-7.322619	0.047946		-7.302308	0.027635
0.500	-7.634547	0.375024	-7.6362483 ^c	-7.372074	0.112552		-7.312484	0.052961		-7.285485	0.025962
1.000	-7.716679	0.511132	-7.66653 ^b	-7.335940	0.130393		-7.263503	0.057956		-7.236899	0.031352
2.000	-7.715709	0.711256	-7.66246 ^b	-7.154170	0.149717		-7.067417	0.062964		-7.038129	0.033676
5.000	-7.002346	1.110399	-6.94230 ^b	-6.068381	0.176434		-5.961689	0.069743		-5.927829	0.035882
5.400	-6.855410	1.151263	-6.8361629 ^c	-5.882659	0.178512		-5.774341	0.070194		-5.740265	0.036118
10.00	-4.684076	1.530623	-4.61777 ^b	-3.348774	0.19532		-3.227581	0.074128		-3.191029	0.037576

TABLE III: Total energies E_{Tot} , ionization energies E_{Ion} , and previously published data E_{Lit} in atomic units for the states $\nu^2 (-1)^+$ ($\nu = 1, 2, 3, 4$) at different field strengths γ .

^aRef. [43]

^bRef. [27]

^cRef. [30]

one order of magnitude to 0.006859 a.u. at $\gamma = 10$.

F. The symmetry subspace $\nu^4 (-1)^-$

In this subsection we will review the results for the quartet states with magnetic quantum number $M = -1$ and negative z -parity, i.e. $\nu^4 (-1)^-$ ($\nu = 1, 2, 3, 4$). In the low field regime ($\gamma < 0.1$) all the curves in Fig. 5 behave similarly: we observe a significant increase of the ionization energies for all considered states of this symmetry subspace. At higher field strengths the energies develop differently for the different states. The one-particle ionization energy of the state $1^4 (-1)^-$ increases monotonously. The ionization energies of the higher ex-

cited states $2^4 (-1)^-$, $3^4 (-1)^-$ and $4^4 (-1)^-$ reach a local maximum for $0.1 < \gamma < 1$. At higher field strengths ($\gamma > 1$) we observe, that the one-particle ionization energies for these states become nearly field independent.

Table V contains the corresponding numerical values. For this symmetry subspace a crossover for the Li^+ threshold state can be observed, as for the $4^4 (-1)^+$ subspace, discussed in the previous subsection.

G. The symmetry subspace $\nu^2 (-2)^+$

In this subsection, we present our results for the $2^2 (-2)^+$ symmetry subspace. Figure 6 shows the curves

		$1^4(-1)^+$			$2^4(-1)^+$		$3^4(-1)^+$		$4^4(-1)^+$	
γ	T_{Sym}	E_{tot}	E_{Ion}	E_{Lit}	E_{tot}	E_{Ion}	E_{tot}	E_{Ion}	E_{tot}	E_{Ion}
0.000	3_0^+	-5.366705	0.256072	-5.35888 ^a	-5.185835	0.075202	-5.149221	0.038588	-5.141528	0.030895
0.001	3_0^+	-5.368015	0.256375	-5.36088 ^a	-5.187601	0.075961	-5.151053	0.039413	-5.143423	0.031783
0.010	3_0^+	-5.385841	0.265227	-5.37871 ^a	-5.205247	0.084633	-5.165602	0.044987	-5.159412	0.038798
0.100	3_0^+	-5.550268	0.345788	-5.54149 ^a	-5.321977	0.117497	-5.278074	0.073594	-5.269906	0.065426
0.200	$3(-1)^+$	-5.703511	0.403056	-5.69451 ^a	-5.416500	0.116045	-5.410188	0.109732	-5.360211	0.059756
0.500	$3(-1)^+$	-6.058463	0.414736	-6.04787 ^a	-5.764438	0.120712	-5.698644	0.054917	-5.670565	0.026839
1.000	$3(-1)^+$	-6.494196	0.374980	-6.48029 ^a	-6.233729	0.114513	-6.172480	0.053263	-6.149065	0.029849
2.000	$3(-1)^+$	-7.206026	0.306258	-7.18889 ^a	-6.997908	0.098140	-6.947211	0.047444	-6.923717	0.023949
5.000	$3(-1)^+$	-8.905985	0.269712	-8.88981 ^a	-8.726111	0.089838	-8.680340	0.044067	-8.650224	0.013952
5.400	$3(-1)^+$	-9.096395	0.268724	-9.0035 ^b	-8.917195	0.089525	-8.861757	0.034086		
10.00	$3(-1)^+$	-10.925976	0.266916	-10.91059 ^a	-10.748366	0.0893068	-10.702625	0.043565	-10.665919	0.006859

TABLE IV: Total energies E_{Tot} , one-particle ionization energies E_{Ion} , and previously published data E_{Lit} in a. u. for the states $\nu^4(-1)^+$ ($\nu = 1, 2, 3, 4$), as well as the threshold symmetry T_{Sym} for different field strengths γ .

^aRef. [27].

^bRef. [26].

$1^4(-1)^-$ $2^4(-1)^-$ $3^4(-1)^-$ $4^4(-1)^-$										
γ	T_{Sym}	E_{tot}	E_{Ion}	E_{Lit}	E_{tot}	E_{Ion}	E_{tot}	E_{Ion}	E_{tot}	E_{Ion}
0.000	3_0^+	-5.243519	0.1328852	-5.24554 ^a	-5.172069	0.0614360	-5.144236	0.0336028	-5.128015	0.0173817
0.001	3_0^+	-5.245744	0.1341042	-5.23386 ^b	-5.174078	0.0624380	-5.146267	0.0346276	-5.133621	0.0219813
0.010	3_0^+	-5.262918	0.1423040	-5.25170 ^b	-5.191736	0.0711218	-5.161532	0.0409179	-5.146381	0.0257669
0.050	3_0^+	-5.339046	0.1799396		-5.257953	0.0988460	-5.210369	0.0512629	-5.192019	0.0329123
0.100	3_0^+	-5.429067	0.2245868	-5.41643 ^b	-5.326415	0.1219344	-5.265077	0.0605963	-5.262003	0.0575226
0.200	$3(-1)^+$	-5.587442	0.2869864	-5.57585 ^b	-5.441002	0.1405464	-5.399005	0.0985497	-5.352709	0.0522539
0.500	$3(-1)^+$	-5.983849	0.3401224	-5.96957 ^b	-5.748951	0.1052242	-5.697593	0.0538666	-5.691942	0.0482154
1.000	$3(-1)^+$	-6.508527	0.3893105	-6.49248 ^b	-6.229901	0.1106850	-6.170544	0.0513275	-6.147671	0.0284546
5.000	$3(-1)^+$	-9.148122	0.5118489	-9.12554 ^b	-8.760873	0.1245998	-8.691638	0.0553655	-8.665490	0.0292174
10.00	$3(-1)^+$	-11.204311	0.5452518	-11.17886 ^b	-10.787789	0.1287291	-10.715697	0.0566372	-10.688192	0.0291328

TABLE V: Total energies E_{Tot} , one-particle ionization energies E_{Ion} , and previously published data E_{Lit} in a. u. for the states $\nu^4(-1)^-$ ($\nu = 1, 2, 3, 4$) and the corresponding threshold symmetry T_{Sym} at different field strengths γ .

^aRef. [27].

^bRef. [26].

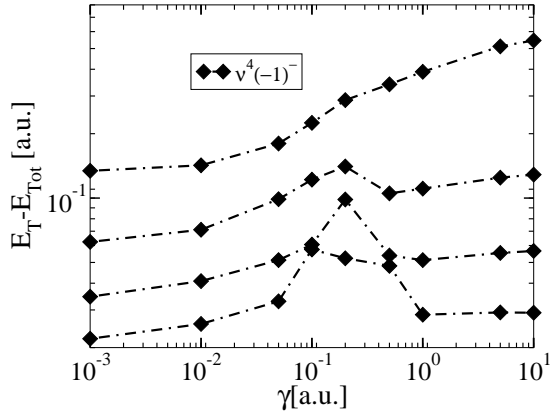


FIG. 5: One-particle ionization energy for the states $\nu^4(-1)^-$ ($\nu = 1, 2, 3, 4$) in a.u. as a function of the magnetic field strength γ .

for the one-particle ionization energy and table VI contains the numerical results for the total energies, one-particle ionization energies as well as previously pub-

lished data. The ground state of this symmetry $1^2(-2)^+$ is a triply tightly bound state. Therefore the one-particle ionization energy increases monotonously. For this state the increase amounts to more than one order of magnitude in the considered range of field strengths. At zero field it is 0.0554 a.u. and at $\gamma = 10$ 1.017 a.u., i.e. an increase by approximately a factor of 20.

For the first excited state of this symmetry ($2^2(-2)^+$) we observe in Fig. 6 an increase, which is less pronounced than for the ground state of the same symmetry. We obtain for its one-particle ionization energy at vanishing field 0.031106 a.u. and at the highest considered field strength ($\gamma = 10$) 0.172684 a.u., which corresponds to an increase of a factor 5.

For the two higher excited states of this symmetry ($3^2(-2)^+$ and $4^2(-2)^+$) the situation is different. In the intermediate field regime again avoided crossings take place. Therefore their one-particle ionization energies pass through local minima at $\gamma \approx 0.1$ ($3^2(-2)^+$) and $\gamma \approx 0.2$ ($4^2(-2)^+$) respectively.

	$1^2(-2)^+$			$2^2(-2)^+$		$3^2(-2)^+$		$4^2(-2)^+$	
γ	E_{tot}	E_{Ion}	E_{Lit}	E_{tot}	E_{Ion}	E_{tot}	E_{Ion}	E_{tot}	E_{Ion}
0.000	-7.332617	0.055426	-7.335523541 ^a	-7.308297	0.031106	-7.297036	0.019845	-7.296823	0.019632
0.001	-7.334097	0.056908		-7.309735	0.032547	-7.297990	0.020801	-7.294566	0.017378
0.010	-7.346296	0.068969		-7.318595	0.041269	-7.306747	0.029421	-7.301231	0.023905
0.050	-7.383648	0.106312		-7.330479	0.053143	-7.314511	0.037175	-7.305505	0.028169
0.100	-7.414207	0.137310	-7.4169780 ^b	-7.339471	0.062574	-7.312327	0.035430	-7.296226	0.019329
0.200	-7.455585	0.180912		-7.349825	0.075152	-7.314596	0.039923	-7.291517	0.016844
0.500	-7.524481	0.264958		-7.353984	0.094462	-7.305925	0.046403	-7.284644	0.025122
1.000	-7.562892	0.357345		-7.316557	0.111010	-7.257044	0.051497	-7.231281	0.025735
5.000	-6.633118	0.741172		-6.045774	0.153827	-5.955127	0.063181	-5.923863	0.031917
5.400	-6.472203	0.768057	-6.451608 ^b	-5.860240	0.156093	-5.768012	0.063865	-5.736691	0.032544
10.00	-4.170890	1.017437		-3.326137	0.172684	-3.221213	0.067760	-3.186407	0.032955

TABLE VI: Total energies E_{Tot} , one-particle ionization energies E_{Ion} , and previously published data E_{Lit} in atomic units for the states $\nu^2(-2)^+$ ($\nu = 1, 2, 3, 4$) at different field strengths γ .

^aRef. [40].

^bRef.[30].

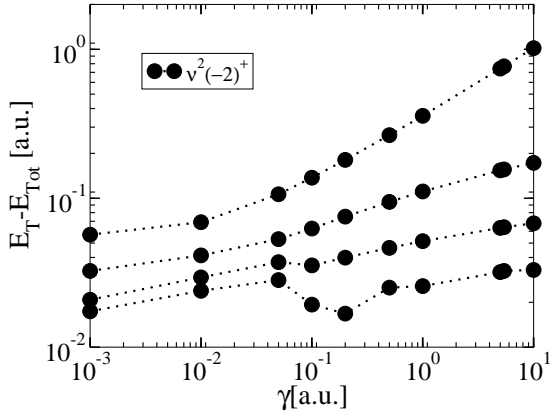


FIG. 6: One-particle ionization energy for the states $\nu^2(-2)^+$ ($\nu = 1, 2, 3, 4$) in a.u. as a function of the magnetic field strength γ .

H. The symmetry subspace $\nu^4(-2)^+$

For the corresponding quadruplet subspace $4(-2)^+$ the ionization energies are shown in Fig. 7 and numerical values are given in table VII. The behavior of the one-particle ionization energies is different compared to the corresponding behavior of the doublet states presented in the previous subsection. At low fields ($\gamma < 0.05$) an increase can be observed for all states considered in this work. For the ground state $1^4(-2)^+$ the one-particle ionization energy increases from 0.06017 a.u. at $\gamma = 0$ to 0.190927 a.u. at $\gamma = 0.2$, where it reaches a local maximum. At this field strength the ionization threshold changes, as for the other quadruplet states. Consequently the ionization energy decreases and passes through a local minimum at $\gamma \approx 1$. At $\gamma \approx 0.5$ an avoided crossing occurs, which leads to an increase of the one-particle ionization energy for the state $1^4(-2)^+$ for higher field strengths. On the other hand, the corresponding energy for the state $2^4(-2)^+$ which increases for $\gamma \gtrsim 0.5$ acquires

a strongly decreasing behavior due to this avoided crossing. Further avoided crossings among the higher excited states cause the states $3^4(-2)^+$ and $4^4(-2)^+$ to become unbound for $\gamma > 1$ ($3^4(-2)^+$) and $\gamma > 0.5$ ($4^4(-2)^+$), respectively. We remark, that there are no previously calculated data on states of the $4(-2)^+$ symmetry in the literature.

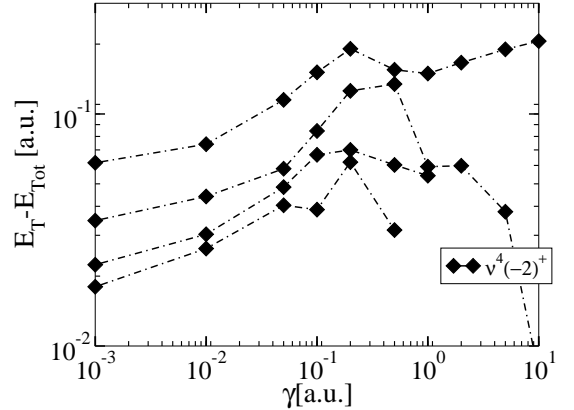


FIG. 7: One-particle ionization energies for the states $\nu^4(-2)^+$ ($\nu = 1, 2, 3, 4$) in a.u. as a function of the magnetic field strength γ .

I. The symmetry subspace $\nu^4(-3)^+$

Let us discuss our results for the symmetry subspace $2S+1M^{\Pi_z} = 4(-3)^+$. The energetically lowest state in this subspace represents the global ground state of the lithium atom in the high field regime, as mentioned above. It is a triply tightly bound state containing a.o. the orbitals $1s2p_{-1}3d_{-2}$. In Fig. 8 it can be seen, that its one-particle ionization energy increases strongly as a function of the field strength. At zero magnetic field it is about 0.03164 a.u., whereas at $\gamma = 10$ an energy

	$1^4(-2)^+$			$2^4(-2)^+$		$3^4(-2)^+$		$4^4(-2)^+$	
γ	T_{Sym}	E_{tot}	E_{Ion}	E_{tot}	E_{Ion}	E_{tot}	E_{Ion}	E_{tot}	E_{Ion}
0.000	$^3_0^+$	-5.170803	0.060170	-5.143875	0.033242	-5.131679	0.021046	-5.124827	0.014194
0.001	$^3_0^+$	-5.173261	0.061621	-5.146306	0.034666	-5.134036	0.022396	-5.129671	0.018031
0.010	$^3_0^+$	-5.194678	0.074063	-5.164667	0.044053	-5.150889	0.030275	-5.146865	0.026251
0.050	$^3_0^+$	-5.274146	0.115039	-5.217208	0.058102	-5.207536	0.048430	-5.199501	0.040395
0.100	$^3_0^+$	-5.355652	0.151172	-5.289006	0.084526	-5.271140	0.066660	-5.243141	0.038661
0.200	$^3(-1)^+$	-5.491382	0.190927	-5.426277	0.125822	-5.370458	0.070003	-5.362501	0.062046
0.500	$^3(-1)^+$	-5.798837	0.155110	-5.778279	0.134552	-5.704042	0.060316	-5.675295	0.031569
1.000	$^3(-1)^+$	-6.268653	0.149437	-6.178554	0.059338	-6.173405	0.054189		
2.000	$^3(-1)^+$	-7.066163	0.166395	-6.959543	0.059775				
5.000	$^3(-1)^+$	-8.826185	0.189912	-8.674211	0.037938				
10.00	$^3(-1)^+$	-10.865122	0.206062	-10.666670	0.007610				

TABLE VII: Total energies E_{Tot} , and one-particle ionization energies E_{Ion} in a.u. for the states $\nu^4(-2)^+$ ($\nu = 1, 2, 3, 4$) and the threshold symmetry T_{Sym} at different field strengths γ .

of 1.3033 a.u. is needed to ionize the state. Therefore the one-particle ionization energy increases roughly by a factor of 40. However, if the reader compares the one-particle ionization energies in table VIII with table III, it is evident that the state $1^4(-3)^+$ is not the state with the highest ionization energy for any field strength.

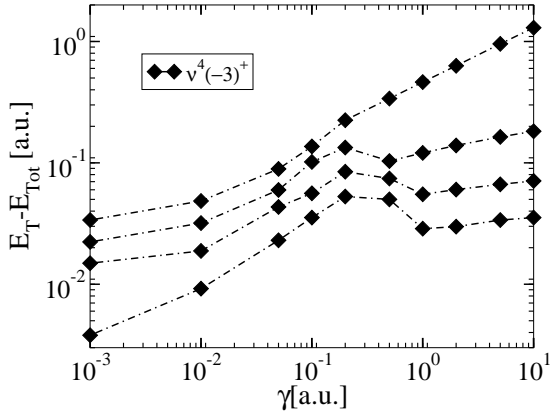


FIG. 8: One-particle ionization energy for the states $\nu^4(-3)^+$ ($\nu = 1, 2, 3, 4$) in a.u. as a function of the magnetic field strength γ .

The ionization energies for the excited states $2^4(-3)^+$, $3^4(-3)^+$ and $4^4(-3)^+$ behave all very similar. Their ionization energy increases up to $\gamma \approx 0.5$, where a local maximum is reached. For $0.5 \gtrsim \gamma \gtrsim 2$ the ionization energy decreases, whereas for higher field strengths it increases again with a lower slope than for $\gamma < 0.5$. Our numerical energy values for the $1^4(-3)^+$ state are always lower than the energies obtained in the literature (see table VIII and Refs. [27, 28]).

V. WAVELENGTHS FOR ELECTROMAGNETIC TRANSITIONS

In this section we present the results for the wavelengths λ of the allowed electric dipole transitions. We will restrict the wavelengths to the regime $\lambda < 10^5$ Å in order to avoid too large uncertainties. In the following we will consider the linear polarized transition $\nu^4(-1)^+ \rightarrow \mu^4(-1)^-$ ($\nu, \mu = 1, 2, 3, 4$) (shown in Fig. 9) and the circular polarized transitions $\nu^{2S+1}M^+ \rightarrow \mu^{2S+1}(M-1)^-$ ($\nu, \mu = 1, 2, 3, 4$) for $(M, S) = (0, 2)$, $(-1, 2)$, $(-1, 4)$, and $(-2, 4)$ in Figs. 10 to 13.

First, we discuss some general features of the transition wavelengths. For the circular polarized transitions $(M, S) = (0, 2)$, $(-1, 2)$, and $(-2, 4)$ (presented in Figs. 10, 11, and 13) it can be observed, that some transition wavelengths decrease in the limit of a strong field, thereby following a power law. Whereas for the linear polarized transition (Fig. 9), and the circular polarized transition $(M, S) = (-1, 4)$ (Fig. 12) such a behavior can not be observed. The transitions, with the strongly decreasing wavelengths are the ones, which involve triply tightly bound states. In our case these are the states $1^2_0^+$, $1^2(-1)^+$, $1^2(-2)^+$ and $1^4(-3)^+$. The corresponding wavelengths become for $\gamma = 10$ shorter than 10^3 Å, whereas the remaining transition wavelengths are in general longer than 10^3 Å. In the symmetry subspaces, involved for the linear polarized transitions considered here, and the circular polarized transitions with $(M, S) = (-1, 4)$, no triply tightly bound states exist.

For the linear polarized transitions $\nu^4(-1)^+ \rightarrow \mu^4(-1)^-$ ($\nu, \mu = 1, 2, 3, 4$) shown in Fig. 9 it can be observed, that the wavelengths in the low field regime ($\gamma < 0.1$) are nearly constant. In the regime $0.1 \leq \gamma \leq 5$ the spectrum of wavelengths becomes very complicated. This is due to avoided crossings of excited states being present in both symmetry subspaces, that are involved in the transitions. Especially we find divergences of the transition wavelengths, being a consequence of crossovers of the energy levels.

In Fig. 10 the transition wavelengths for the circular

		$1^4(-3)^+$			$2^4(-3)^+$		$3^4(-3)^+$		$4^4(-3)^+$	
γ	T_{Sym}	E_{tot}	E_{Ion}	E_{Lit}	E_{tot}	E_{Ion}	E_{tot}	E_{Ion}	E_{tot}	E_{Ion}
0.000	$^3_0^+$	-5.142319	0.031686	-5.08379 ^a	-5.125979	0.015346				
0.001	$^3_0^+$	-5.145464	0.033824	-5.08679 ^a	-5.133945	0.022305	-5.126540	0.014901	-5.115403	0.003764
0.010	$^3_0^+$	-5.169111	0.048497	-5.11268 ^a	-5.152521	0.031907	-5.139446	0.018831	-5.129767	0.009153
0.050	$^3_0^+$	-5.248206	0.089099		-5.218924	0.059818	-5.202450	0.043344	-5.182078	0.022972
0.100	$^3_0^+$	-5.341030	0.136549	-5.32140 ^a	-5.306295	0.101815	-5.260565	0.056085	-5.239866	0.035386
0.200	$^3_{(-1)}^+$	-5.524939	0.224483	-5.51151 ^a	-5.434168	0.133713	-5.384936	0.084481	-5.353290	0.052835
0.500	$^3_{(-1)}^+$	-5.982253	0.338527	-5.97952 ^b	-5.747212	0.103486	-5.717997	0.074271	-5.693685	0.049959
1.000	$^3_{(-1)}^+$	-6.582361	0.463144	-6.57081 ^a	-6.240001	0.120785	-6.174336	0.055119	-6.147905	0.028689
2.000	$^3_{(-1)}^+$	-7.530125	0.630357	-7.52003 ^a	-7.038917	0.139149	-6.959997	0.060229	-6.929553	0.029786
5.000	$^3_{(-1)}^+$	-9.591769	0.955496	-9.57694 ^a	-8.799910	0.163637	-8.702726	0.066453	-8.670060	0.033787
10.00	$^3_{(-1)}^+$	-11.957294	1.298234	-11.93902 ^a	-10.841017	0.181957	-10.730105	0.071045	-10.694481	0.035421

TABLE VIII: Total energies E_{Tot} , one-particle ionization energies E_{Ion} , and previously published data E_{Lit} in a.u., as well as, threshold symmetry T_{Sym} for the states $\nu^4(-3)^+$ ($\nu = 1, 2, 3, 4$) at different field strengths γ .

^aRef. [27].

^bRef. [28].

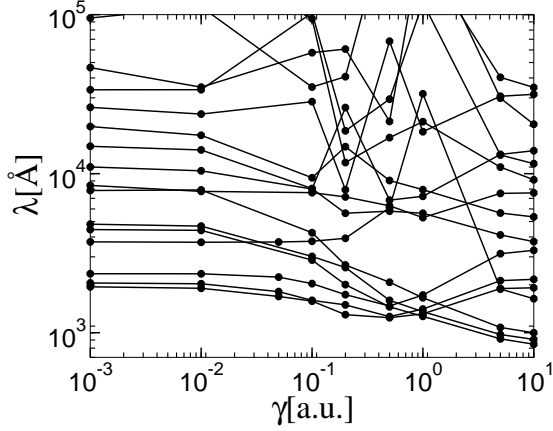


FIG. 9: Transition wavelengths λ for the linear polarized transitions $\nu^4(-1)^+ \rightarrow \mu^4(-1)^-$ ($\nu, \mu = 1, 2, 3, 4$) in Å as a function of the magnetic field strength γ .

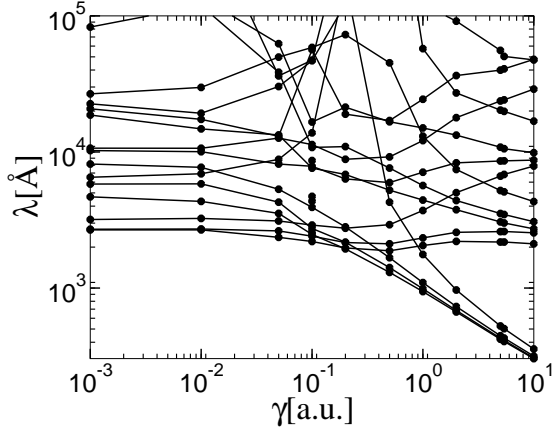


FIG. 10: Transition wavelengths λ for the circular polarized transitions $\nu^2 0^+ \rightarrow \mu^2(-1)^+$ ($\nu, \mu = 1, 2, 3, 4$) in Å as a function of the magnetic field strength γ .

polarized transitions of the form $\nu^2(0)^+ \rightarrow \mu^2(-1)^+$ ($\nu, \mu = 1, 2, 3, 4$) are shown. In the high field limit a bunch of small wavelengths, described above, can be identified easily. These are transitions of the form $\nu^2 0^+ \rightarrow 1^2(-1)^+$, i.e. those involving the state $1^2(-1)^+$. One of these lines diverges at $\gamma \approx 0.2$. It is associated with the transition $1^2 0^+ \rightarrow 1^2(-1)^+$. As mentioned above, the energies of these two states become equal at $\gamma = 0.1929$. Further divergencies can be observed, which are caused by the fact, that energy levels of the $M^{\Pi_z} = -1^+$ symmetry subspace increase much faster as a function of γ , than those belonging to the $M^{\Pi_z} = 0^+$ subspace.

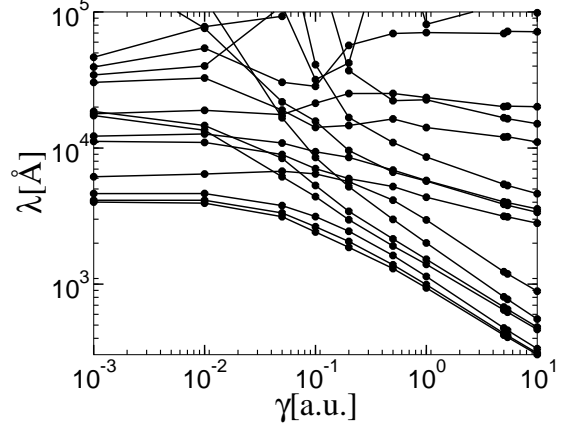


FIG. 11: Transition wavelengths λ for the circular polarized transitions $\nu^2(-1)^+ \rightarrow \mu^2(-2)^+$ ($\nu, \mu = 1, 2, 3, 4$) in Å as a function of the magnetic field strength γ .

For the case of the circular polarized doublet transitions $\nu^2(-1)^+ \rightarrow \mu^2(-2)^+$ ($\nu, \mu = 1, 2, 3, 4$), displayed in Fig. 11, the reader observes eight lines, decreasing in the limit of strong fields thereby following a power law. These lines correspond to the transitions involving the triply tightly bound states $1^2(-1)^+$ and $1^2(-2)^+$. Fur-

thermore the reader should note, that the transitions among the other states show little variation, compared to the transitions $\nu^2 0^+ \rightarrow \mu^2 (-1)^+$, which is a consequence of the fact, that the energy levels in the participating symmetry subspaces behave in a very similar way.

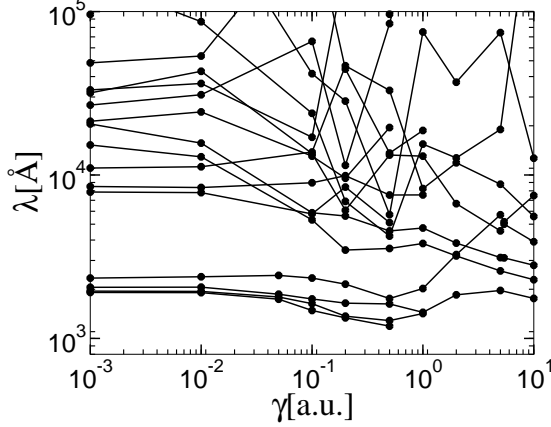


FIG. 12: Transition wavelengths λ for the circular polarized transitions $\nu^4(-1)^+ \rightarrow \mu^4(-2)^+$ ($\nu, \mu = 1, 2, 3, 4$) in Å as a function of the magnetic field strength γ .

The corresponding quadruplet transitions $\nu^4(-1)^+ \rightarrow \mu^4(-2)^+$ ($\nu, \mu = 1, 2, 3, 4$) depicted in Fig. 12 follow a completely different pattern. Because there are no triply tightly bound states in neither of the subspaces, all the wavelengths are longer than 10^3 Å. On the other hand the behavior of the wavelengths in the regime $\gamma > 0.1$ reflects the complicated energy level scheme of both symmetry subspaces, which is dominated by several avoided crossings. They result in energy level crossovers and therefore divergencies for the corresponding wavelengths.

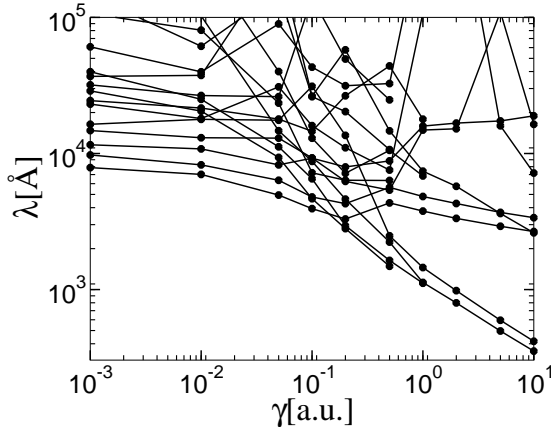


FIG. 13: Transition wavelengths λ for the circular polarized transitions $\nu^4(-2)^+ \rightarrow \mu^4(-3)^+$ ($\nu, \mu = 1, 2, 3, 4$) in Å as a function of the magnetic field strength γ .

For the transitions $\nu^4(-2)^+ \rightarrow \mu^4(-3)^+$ ($\nu, \mu =$

1, 2, 3, 4) shown in Fig. 13 one observes some very short transition wavelengths at $\gamma = 10$ ($\lambda < 400$ Å), that correspond to transitions involving the high field ground state $1^4(-3)^+$, which is a triply tightly bound state. For $\gamma > 0.1$ avoided crossings and the rearrangement of energy levels creates a complex pattern.

VI. SUMMARY AND CONCLUSIONS

In the present work we have investigated the electronic structure of the lithium atom exposed to a strong homogeneous magnetic field. We cover the broad regime of field strengths $0 \leq \gamma \leq 10$ providing data for a grid of ten values for the field strength. The key ingredient of our computational method is an anisotropic Gaussian basis set whose nonlinear variational parameters (exponents!) are optimized for each field strength. These nonlinear optimizations, being based on a sophisticated algorithmic procedure, are performed for *one- and two-electron atomic systems* in the presence of the field. As a result we obtain a basis set of orbitals that allows for a rapidly convergent numerical study of the electronic structure of, in particular, the lithium atom.

Our computational approach to the three-electron problem is a full configuration interaction method. This approach yields fully correlated wave functions that can, in principle, be determined to arbitrary accuracy. To implement it for the above-mentioned basis set a number of techniques had to be combined. To avoid linear dependencies of our non-orthogonal orbitals a cut-off technique with respect to the overlap and Hamiltonian configuration matrix has been employed. Employing large configurational basis sets of the order of several ten-thousand we arrived at relative accuracies of the order of 10^{-4} for the total energies of the lithium atom in the presence of the field.

Total and one-particle ionization energies as well as transition wave lengths have been calculated for the ground and typically three excited states for each of the symmetries $2^0+, 2^2(-1)^+, 4^4(-1)^+, 4^4(-1)^-, 2^2(-2)^+, 4^4(-2)^+, 4^4(-3)^+$ thereby yielding a total of 28 states. This has to be compared with the existing data on the lithium atom in the literature where only a few states for a few field strengths have been investigated previously. Also, the predominant part of these investigations were not on a fully correlated level.

The ground state crossovers of the lithium atom with increasing field strength were redetermined thereby yielding more precise values for the crossover field strengths. A classification and discussion of the one-electron ionization energies for the ground and excited states for each of the above-given symmetries has been provided. Particular emphasis has been given to the effects due to the tightly bound orbitals and the singly or multiply tightly bound configurations. Only a very limited number of states show a monotonically increasing one-electron ion-

ization energy in the complete regime of field strengths considered here. With increasing degree of excitation avoided crossings lead to a nonmonotonous behavior of the energies. For the electromagnetic transitions that involve states with tightly bound orbitals we observe bundles of short wavelengths that decrease monotonically

with increasing field strength.

In principle our approach allows investigations of more than three electron atoms. Furthermore since it yields the eigenfunctions arbitrary properties and in particular oscillator strengths for lithium and more electron atoms can be obtained.

-
- [1] H. Friedrich and D. Wintgen, Phys. Rep. **183**, 37 (1989).
 - [2] H. Ruder, G. Wunner, H. Herold, and F. Geyer, *Atoms in Strong Magnetic Fields* (Springer, Heidelberg, 1994).
 - [3] L. S. Cederbaum, K. C. Kulander, and N. H. March, eds., *Atoms and Molecules in Intense Fields*, vol. 86 of *Structure and Bonding* (Springer, 1997).
 - [4] P. Schmelcher and W. Schweizer, eds., *Atoms and Molecules in Strong External Fields* (Plenum Press, New York, 1998).
 - [5] F. Herlach and N. Miura, eds., *High magnetic fields, Science and Technology, Theory and Experiments I*, vol. 2 (World Scientific, 2003).
 - [6] N. Merani, J. Main, and G. Wunner, Astr. & Astrophys. **298**, 193 (1995).
 - [7] J. Angel, J. Liebert, and H. S. Stockmann, Astrophys. J. **292**, 260 (1985).
 - [8] J. Angel, Ann. Rev. Astron. Astrophys. **16**, 487 (1978).
 - [9] J. L. Greenstein, R. Henry, and R. F. O'Connell, Astrophys. J. **289**, L25 (1985).
 - [10] G. Wunner, W. Rösner, H. Herold, and H. Ruder, Astron. Astrophys. **149**, 102 (1985).
 - [11] D. T. Wickramasinghe and L. Ferrario, Astrophys. J. **327**, 222 (1988).
 - [12] W. Becken, P. Schmelcher, and F. Diakonos, J. Phys. B **32**, 1557 (1999); W. Becken and P. Schmelcher, J. Phys. B **33**, 545 (2000); Phys. Rev. A **63**, 053412 (2001), **65**, 033416 (2002).
 - [13] O.-A. Al-Hujaj and P. Schmelcher, Phys. Rev. A **67**, 023403 (2002), **68**, 053403 (2003).
 - [14] R. F. Green and J. Liebert, Publ. Astr. Soc. Pac. **93**, 105 (1980).
 - [15] G. D. Schmidt, W. B. Latter, and C. B. Foltz, Astrophys. J. **350**, 768 (1990).
 - [16] G. D. Schmidt, R. G. Allen, P. S. Smith, and J. Liebert, Astrophys. J. **463**, 320 (1996).
 - [17] S. Jordan, P. Schmelcher, W. Becken, and W. Schweizer, Astron. Astrophys. Lett. **336**, L33 (1998).
 - [18] S. Jordan, P. Schmelcher, and W. Becken, Astron. Astrophys. **376**, 614 (2001).
 - [19] G. D. Schmidt, S. Vennes, D. T. Wickramasinghe, and L. Ferrario, Mon. Not. R. Astron. Soc. **332**, 29 (2002).
 - [20] D. T. Wickramasinghe and L. Ferrario, Pub. Astron. Soc. Pac. **112**, 873 (2000).
 - [21] D. Reimers, S. Jordan, V. Beckmann, N. Christlieb, and L. Wisotzki, Astron. & Astrophys. **337**, L13 (1998).
 - [22] H. H. G. Schmidt and J. Liebert, preprint.
 - [23] I. N. Reid, J. Liebert, and G. D. Schmidt, Astrophys. J. **550**, L61 (2001).
 - [24] D. Neuhauser, S. E. Koonin, and K. Langanke, Phys. Rev. A **36**, 4163 (1987).
 - [25] M. Demeur, P.-H. Heenen, and M. Godefroid, Phys. Rev. A **49**, 176 (1994).
 - [26] M. D. Jones, G. Ortiz, and D. M. Ceperley, Phys. Rev. A **54**, 219 (1996).
 - [27] M. V. Ivanov and P. Schmelcher, Phys. Rev. A **57**, 3793 (1998).
 - [28] M. Ivanov and P. Schmelcher, Phys. Rev. A **61**, 022505 (2000).
 - [29] H. Qiao and B. Li, Phys. Rev. A **62**, 0033401 (2000).
 - [30] X. Guan and B. Li, Phys. Rev. A **63**, 043413 (2001).
 - [31] K. Mori and C. J. Hailey, Astrophys. J. **564**, 914 (2002).
 - [32] P. Schmelcher and L. S. Cederbaum, Phys. Rev. A **37**, 672 (1988).
 - [33] U. Kappes and P. Schmelcher, Phys. Rev. A **54**, 1313 (1996), **53**, 3869 (1996); **51**, 4542 (1995).
 - [34] T. Detmer, P. Schmelcher, F.K. Diakonos, and L. Cederbaum, Phys. Rev. A **56**, 1825 (1997); T. Detmer, P. Schmelcher, and L. Cederbaum, Phys. Rev. A **57**, 1767 (1998); **61**, 043411 (2000); **64**, 023410 (2001); J. Chem. Phys., **109** (1998); J. Phys. B **28** (1995).
 - [35] A. Szabo and N. S. Ostlund, *Modern quantum chemistry* (Dover Publications, Mineola, New York, 1996).
 - [36] O.-A. Al-Hujaj and P. Schmelcher, Phys. Rev. A **61**, 063413 (2000).
 - [37] M. V. Ivanov and P. Schmelcher, Phys. Rev. A **60**, 3558 (1999).
 - [38] M. Ivanov and P. Schmelcher, Eur. Phys. J. D **14**, 279 (2001).
 - [39] M. V. Ivanov and P. Schmelcher, J. Phys. B **34**, 2031 (2001).
 - [40] Z.-C. Yan and G. Drake, Phys. Rev. A **52**, 3711 (1995).
 - [41] F. W. King, Phys. Rev. A **43**, 3285 (1991).
 - [42] J. Pipin and D. M. Bishop, Phys. Rev. A **45**, 2736 (1992).
 - [43] J. S. Sims and S. A. Hagstrom, Phys. Rev. A **11**, 418 (1975).